# Protein Macroarray Profiling of Serum Autoantibodies in Pseudoexfoliation Glaucoma

*Edward W. Dervan,[1] Hong Chen,[2] Su Ling Ho,[1] Nikola Brummel,[2] Jasmin Schmid,[2] David Toomey,[2] Margarita Haralambova,[2] Edith Gould,[2] Deborah M. Wallace,[1] Jochen H. M. Prehn,[2] Colm J. O'Brien,[1,3] and Derek Murphy[2]*

**Purpose.** Complex repertoires of IgG autoantibodies have been detected against ocular antigens in patients with glaucoma. The goal was to identify and characterize the IgG autoantibody repertoires in sera of patients with pseudoexfoliation glaucoma (PXFG) with protein macroarrays.

**Methods.** Serum samples of 21 patients with PXFG and 19 age- and sex-matched control subjects were profiled on high-density colony protein macroarrays expressing His-tagged recombinant human proteins derived from a human fetal brain cDNA library. Statistically prevalent expression clones in the PXFG group were sequenced. mRNA expression of identified antigens was examined in the rat ganglion cell line RGC-5 and in human brain and optic nerve cDNA. The IgG immunoreactivity of the sera of 20 control and 26 PXFG patients to purified C6orf129 was analyzed in a reverse enzyme-linked immunosorbent assay.

**Results.** An increased prevalence was detected among the PXFG patients of serum antibodies to seven proteins: C6orf129; stathmin-like 4; transmembrane protein 9 domain family, member B; fibroblast growth factor receptor 3; cleft lip and palate transmembrane protein 1; EH-domain-containing protein 1; and eukaryotic translation elongation factor 2. All antigens were expressed in the RGC-5 cells and in cDNA from human brain and optic nerve, with the exception of stathmin-like 4, which was not expressed in the RGC-5 cells. The patients with PXFG had increased anti-C6orf129 IgG immunoreactivity compared with that in the control subjects ($P < 0.05$).

**Conclusions.** Screening high-density protein arrays identifies unique antibody profiles that may discriminate between patients with and without PXFG. Characterization of the autoantibody repertoire may provide new insights into the pathophysiology of PXFG. (*Invest Ophthalmol Vis Sci.* 2010;51:2968–2975) DOI:10.1167/iovs.09-4898

From the [1]Institute of Ophthalmology, Mater Misericordiae University Hospital, Dublin, Ireland; the [2]Centre for Human Proteomics, Royal College of Surgeons in Ireland, Dublin, Ireland; and the [3]Conway Institute of Biomolecular and Biomedical Research, University College Dublin, Dublin, Ireland.

Supported by a grant from the Glaucoma Foundation, New York.

Submitted for publication November 11, 2009; revised January 1, 2010; accepted January 10, 2010.

Disclosure: **E.W. Dervan**, None; **H. Chen**, None; **S.L. Ho**, None; **N. Brummel**, None; **J. Schmid**, None; **D. Toomey**, None; **M. Haralambova**, None; **E. Gould**, None; **D.M. Wallace**, None; **J.H.M. Prehn**, None; **C.J. O'Brien**, None; **D. Murphy**, None

Corresponding author: Edward W. J. Dervan, Institute of Ophthalmology, Mater Misericordiae University Hospital, Dublin 7, Ireland; edervan@mac.com.

Glaucoma is a leading cause of irreversible blindness that will affect an estimated 60 million people worldwide by 2010.[1,2] It is a chronic neurodegenerative disease characterized by the slow progressive death of retinal ganglion cells and their axons. Pseudoexfoliation (PXF) syndrome is currently the single most important identifiable risk factor for open-angle glaucoma.[3] PXF is a generalized disorder of the extracellular matrix characterized by the production and progressive accumulation of fibrillar material in tissues throughout the anterior segment and in the connective tissue portions of the various visceral organs. PXF has a higher frequency of severe optic nerve damage at the time of diagnosis and is more resistant to medical therapy than is primary open-angle glaucoma.[4] Furthermore, PXF has been associated with a higher incidence of cardiovascular events and some other neurodegenerative disorders, including Alzheimer's disease and sensorineural deafness.[5–8] A recent genome-wide association study in the Icelandic population identified multiple single-nucleotide polymorphisms in the lysyl oxidase-like 1 (*LOXL1*) gene on 15q24.1 that are highly associated with the exfoliation phenotype.[9]

There is a growing body of evidence indicating that a neuroinflammatory response is involved in the pathologic cascade of retinal ganglion cell death.[10] A significant fraction of genes with modified expression in gene array analysis in experimental models of glaucoma are associated with inflammation and the immune response.[11–13] Chronic activation of glial cells (microglia and astrocytes) is seen in glaucomatous human eyes,[14] with accompanying upregulation of major histocompatibility complex class I and II antigens, indicating the activation of their antigen-presenting ability.[15,16] Expansion and secondary recruitment of circulating T-cells through this process is supported by evidence of abnormal T-cell subsets[17] and increased production of serum autoantibodies to ocular proteins.[18] This activated immune response in glaucoma may be partly associated with the increased expression and exposure of neuronal antigens as a result of neuronal stress and injury. The activation of specific autoimmune responses may be detrimental, but may have a physiological role in protecting the damaged optic nerve.[10,18]

Complex repertoires of IgG autoantibodies have been detected against retinal, optic nerve, and optic nerve head antigens in patients with primary open-angle glaucoma (POAG), normal tension glaucoma (NTG), and ocular hypertension (OHT) by means of sodium dodecyl sulfate-polyacrylamide gel electrophoresis (SDS-PAGE).[19,20] Identification of the immunoreactive bands by mass spectrometry has identified several target antigens including heat shock proteins,[21,22] glutathione *S*-transferase,[23] α-fodrin,[24] γ-enolase,[25] glycosaminoglycans,[26] myelin basic protein,[27] histone H4,[28] and cellular retinaldehyde-binding protein.[28] Although the pathogenic role of these antibodies is unclear, characterizing this antibody repertoire may provide insights into the aberrant cellular mechanisms in

glaucoma development, ultimately leading to novel diagnostic or therapeutic targets.

We have taken the novel approach of screening colony macroarrays containing more than 10,000 different human proteins, to detect disease-associated serum autoantibodies in patients with PXF glaucoma (PXFG).[29] The thousands of proteins on the array act as capture antigens, enabling the detection of glaucoma-associated autoantibody signatures. This approach has been applied to the detection of autoantibody signatures in several diseases, including colorectal cancer and dilated cardiomyopathy, revealing panels of disease-associated autoantibody biomarkers.[30–32] The purpose of this study was to analyze and compare the serum autoantibody profiles of patients with and those without PXFG to identify glaucoma-associated autoantibodies.

## METHODS

### Patients

The study population consisted of two groups: patients with PXFG, and age- and sex-matched control subjects (volunteers without any ocular disorder). All patients had a complete ophthalmic examination at the Ophthalmology Department, Mater Misericordiae University Hospital, Dublin, Ireland. The investigation was conducted in accordance with the tenets of the Declaration of Helsinki. Informed consent was obtained from the subjects after explanation of the nature and possible consequences of the study. Blood samples were obtained according to a protocol that was approved by the Research Ethics Committee of the Mater Misericordiae University Hospital.

The patient classification was in accordance with the guidelines of the European Glaucoma Society.[33] The diagnosis of PXFG was defined by the presence of characteristic PXF material on the iris or lens capsule and evidence of glaucoma. For control purposes, we used serum from patients attending for cataract surgery. In the control patients, PXF was excluded by the absence of PXF material and glaucoma. All patients included in the study had no known history of autoimmune disease, diabetes mellitus, or other ocular disorder. After the participants supplied informed, written consent, blood samples were obtained. After centrifugation at 8000 rpm for 15 minutes at 4°C, the sera were collected and stored at −80°C for later examination.

### Protein Arrays

Serum from 21 patients with PXFG and 19 control subjects were screened by using high-density colony macroarrays (ImaGenes, Berlin, Germany). The cDNA library of human fetal brain (hEX1) was cloned in pQE30NST and used to transform *Escherichia coli* SCS1 (Stratagene, La Jolla, CA).[34] This method allows the expression of His6-tagged fusion proteins in the presence of isopropyl β-D-1-thiogalactopyranoside (IPTG). In total, 37,830 clones expressing recombinant human proteins were used for the generation of the high-density protein arrays.[29,34] The clones are spotted on the array in an ordered fashion that allows for easy identification and further characterization. Not all the clones express a different protein, with some expressing different sized fragments of the same protein. However, the array contains approximately 10,000 unique proteins.

To identify IgG antibodies in the serum of patients, we prepared the arrays as previously described.[29,31] Briefly, hEx1 protein arrays were incubated with diluted serum (1:100) for 16 hours. Mouse anti-human IgG antibody (GG-7; Sigma-Aldrich, St. Louis, MO), alkaline phosphatase-conjugated goat anti-mouse IgG antibody (A1418, Sigma-Aldrich) and a substrate (AttoPhos; JBL Scientific, San Luis Obispo, CA) were used as detection reagents. Images were captured with a high-resolution CCD detection system (LAS3000; Fujifilm, Tokyo, Japan).

Images were analyzed for signal intensity (VisualGrid; GPC Biotech, Martinsried, Germany). The position of each clone on the array is contained within the software. This enables correlation of the identified positives with the corresponding clone identifications. Each clone is spotted on the array in duplicate in a specific 5 × 5 pattern. The arrays were scored on the presence or not of matched duplicates (Supplementary Fig. S1, http://www.iovs.org/cgi/content/full/51/6/2968/DC1). After analysis, a unique antibody profile for each serum sample is generated. The clones identified in this analysis were then compared between patients with PXFG and control subjects.

### Sequencing and Analysis of cDNA inserts

Plasmid DNA was isolated for DNA sequencing (QIAprep spin Miniprep kit; Qiagen, Venlo, The Netherlands) according to the manufacturer's instructions. Cloned cDNAs in the purified plasmid DNA were sequenced by Agowa Genomics Services (Berlin, Germany) using the primers pQE-F (5′-CGGATAACAATTTCACACAG-3′) and pQE-R (5′-GTTCTGAGGTCATTACTGG-3′). Nucleotide and translated amino acid sequences were compared with known sequences using BLAST algorithms (National Center for Biotechnology Information, Bethesda, MD).[35]

### Protein Expression of the Clone Expressing C6orf129

The *E. coli* containing the clone was plated on 2× YT agar containing 100 μg/mL ampicillin and kanamycin and grown overnight at 37°C. A single colony was then used to inoculate 5 mL of 2× YT containing the same antibiotics as above and incubated overnight at 37°C and 250 rpm. This culture was used to inoculate 1 L of the same medium and was incubated at 37°C and 250 rpm until an $OD_{600nm}$ of approximately 0.6 was reached. IPTG was added to a final concentration of 1.0 mM, and the cultures were incubated at 37°C for 4 hours at 250 rpm. The cells were pelleted by centrifugation at 10,000*g* for 10 minutes at 4°C and stored at −80°C.

The recombinant proteins were extracted by thawing the cell pellets on ice and resuspending them in sterile filtered buffer NPI-10 (50 mM $NaH_2PO_4$, 300 mM NaCl, 10 mM imidazole [pH 8.0]), with RNase A (10 μg/mL), DNase I (5 μg/mL), lysozyme (10 mg/mL; Sigma-Aldrich), and 100× protease inhibitor (Roche Diagnostics, Mannheim, Germany) at 4 mL/g wet weight and incubated on ice for 15 minutes. The resuspended pellets were sonicated on ice with a microtipped sonicator in five 20-second bursts at 250 W with a 20-second cooling period between each burst. Insoluble debris was removed by centrifugation at 10,000*g* for 25 minutes at 4°C. The supernatant containing the protein was used for further purification by fast-performance liquid chromatography (ÄKTA FPLC; GE Healthcare, Buckinghamshire, UK), under the manufacturer's recommended conditions.

### FPLC Purification

The soluble supernatant was purified with $Ni^{2+}$ affinity chromatography, ion exchange, and gel filtration chromatography. The supernatant was loaded onto a 1-mL FF crude column (HisTrap; GE Healthcare) that was equilibrated with 10 column washes with buffer NPI-10. The column was washed with sterile filtered buffer NPI-20 (50 mM $NaH_2PO_4$, 300 mM NaCl, and 20 mM imidazole [pH 8.0]) until the $A_{280nm}$ returned to the baseline value. The bound protein was eluted in 250-μL fractions with sterile filtered buffer NPI 250 (50 mM $NaH_2PO_4$, 300 mM NaCl, and 250 mM imidazole [pH 8.0]) over five column volumes at a flow rate of 1.0 mL/min.

The low-molecular-weight contaminants were removed by combining the eluted fractions from the $Ni^{2+}$ affinity chromatography containing the protein, as determined by SDS-PAGE, and desalting them (HiTrap Desalting Column; GE Healthcare). After equilibration of the column with 25 mL PBS buffer at 5 mL/min, the sample was loaded onto the column. The protein was eluted in 0.5-mL fractions, at a flow rate of 1.0 mL/min, and monitored by absorbance at 280 nm.

After identification by SDS-PAGE, the target fractions were concentrated by ultrafiltration with a centrifugal filter unit (Microcon YM-10; Millipore, Billerica, MA). The protein was loaded for final purification (Superdex 200 column; 1.0 × 30 cm, GE-Healthcare) and equilibrated in PBS. The protein was eluted in 250-μL fractions, at a flow rate of 0.7

**TABLE 1.** Oligonucleotides Primers Used for Real-Time PCR

| Target Gene | | Sequence (5′-3′) | Product Size (bp) |
|---|---|---|---|
| C6orf129 human | F | AGGAGGTCCCTGGAGAAGGAGAAA | 116 |
| | R | ATGGCCACAGAGAGCAGCATGT | |
| C6orf129 rat | F | AAAGAAGCGGGAGAATCTTGGCGT | 173 |
| | R | AGGCTTTGTTCATGAGGGCGTT | |
| Stmn4 human | F | AGCAAGGGTCATGTTTCTGG | 117 |
| | R | AGCAGCTCGCTTCTAACTGG | |
| Stmn4 rat | F | ACCAGATTCCAGCCAACATGACCCT | 144 |
| | R | ACTGTCTCCCACACCAGCCTTCATA | |
| Tmem9b human | F | ATGGGCTCCACAACATGAAG | 124 |
| | R | CCAAGAATTTCGAGGATGTCA | |
| Tmem9b rat | F | GCACGCACCGCAGAATTTTGAA | 138 |
| | R | ACAGGCATTGGCTCCACAACAT | |
| Fgfr3 human | F | ACAGCTCAGCTCCACAGCAT | 117 |
| | R | GAGTCCTTGGGGACGGAG | |
| Fgfr3 rat | F | TGTGCCACTTTAGTGTGCGTGT | 136 |
| | R | GGCACAGCCAGCAGTTTCTTATCCA | |
| Clptm1 human | F | GCGGAACCAACTGCTGAT | 112 |
| | R | GGAGACCCAGCCTCAGAAC | |
| Clptm1 rat | F | AGGTGACCAGCAATGGCAGCAT | 144 |
| | R | AGCTGCTGATGGCCCAGATGAT | |
| Ehd1 human | F | AAGAGCAGGATGATGCGGT | 96 |
| | R | CCTGTCTGGAGAGAAGCAGC | |
| Ehd1 rat | F | CCTTCTTGAGGGAGCTGATG | 319 |
| | R | GAGGACAAGATCCGTGTGGT | |
| Eef2 human | F | GACTTGGAGAGGCAGAGCAC | 125 |
| | R | CTGGAGATCTGCCTGAAGGA | |
| Eef2 rat | F | TTTGAGAATCCGACGCCATCTGCC | 151 |
| | R | TGCACACAAGGGAGTCGGTCAA | |

mL/min and monitored by absorbance at 280 nm. The eluted fractions were analyzed on Coomassie-stained 15% SDS-PAGE gels and the concentration of soluble protein was determined (BCA Protein Assay Kit; Pierce, Rockford, IL).

## SDS-PAGE Analysis

SDS-PAGE was performed with a gel system (Mini-PROTEAN II; Bio-Rad, Hemel Hempstead, UK), to determine the purity and relative molecular weight of the purified protein. The proteins were stained with Coomassie blue G-250.

## Enzyme-Linked Immunosorbent Assay

Detection of antibodies to the purified recombinant human C6orf129 in the sera of 26 patients with PXFG (12 from protein array study and 14 new patients) and 20 control patients (12 from protein array study and 8 new patients) was performed with a direct enzyme-linked immunosorbent assay (ELISA). The purified protein (100 $\mu$L at 7.5 $\mu$g/mL) was added to 48 wells of a 96-well high-binding-capacity plate (HisGrab Copper Coated; Thermo Scientific, Waltham, MA) and incubated at room temperature for 1.5 hours. The plates were washed with PBS containing 0.1% Tween 20 (PBS-T), blocked for 1 hour with PBS-T containing 3% BSA, then washed six times in PBS-T. A 100-$\mu$L aliquot of each serum sample diluted 1:10 with PBS-T containing 0.1% BSA was added to a well that was coated with antigen and a well that was not and incubated for 1.5 hours. The plates were washed six times with PBS-T followed by the addition of 100 $\mu$L of HRP-conjugated polyclonal rabbit anti-human IgG (IS512; DakoCytomation, Hamburg, Germany) diluted 1:5000 in PBS-T. The plates were then incubated at room temperature for a further 1 hour. They were washed six times in PBS-T, and 100 $\mu$L of 2,2′-azino-bis[3-ethylbenzthiazoline-6-sulfonic acid] (ABTS; Calbiochem, Schwalbach, Germany) was added for 30 minutes at room temperature. Signals were measured at 405 nm with a microplate reader. The results for each serum sample were expressed by subtracting the reactivities of the well containing no antigen from those of the well containing the antigen.

## Cell Culture

The RGC-5 cell line is a rat retinal ganglion cell line transformed by an adenovirus carrying early region 1A (E1A). Cells were incubated at 37°C in 5% $CO_2$ in Dulbecco's modified Eagle's medium, supplemented with 10% heat-inactivated fetal calf serum and 1% penicillin/streptomycin (Sigma-Aldrich). For all cell cultures, experiments were maintained at 70% to 80% confluence. The RGC-5 cell line was generously provided by Neeraj Agarwal (North Texas Health Science Center, Fort Worth, TX).

## RNA Extraction and Real-Time Polymerase Chain Reaction

The cells were grown as just detailed, and total RNA was extracted (TRI-reagent; Sigma-Aldrich) per the manufacturer's instructions. Conversion of mRNA to cDNA was achieved by reverse transcription with enhanced avian reverse transcriptase (eAMV; Sigma-Aldrich). First-strand cDNA of brain (C1234035) and optic nerve (C1234064–10) tissue of healthy young male donors was obtained from Biochain (Hayward, CA). The cDNA was then assayed in triplicate (Rotorgene 3000 Real Time PCR system; Corbet, Research, Australia) and the real-time PCR amplification kit (SYBR Green I; Qiagen). Briefly, 1 $\mu$L of cDNA template was mixed with 6.25 $\mu$L SYBR green master mix containing *Taq* and dNTPs (Qiagen), 4.25 $\mu$L DNase-free water and 0.5 $\mu$L each of forward and reverse primers (10 $\mu$M), to give a final volume of 12.5 $\mu$L. Specific custom made primers (Sigma-Aldrich) were designed, ensuring that the primers spanned an exon–exon bridge. The primer sequences are shown in Table 1. The primers were checked on BLAST to ensure that they were specific for their targets. The PCR products were separated on 2% agarose gels and visualized under UV light with a gel-imaging system (Mini BusPro; DNR Bioimaging Systems, Jerusalem, Israel).

## Statistical Analysis

In the analysis of the arrays, Fisher's two-sided exact test was used to compare frequencies of each identified antigen in PXFG and control

**TABLE 2.** PXFG Associated Antigens Identified Using Protein Macroarrays

| Protein Name | Gene Symbol | Ascension Number | Chromosome | Cellular Location | Function | mRNA Expression* | Protein Expression† | PXFG ($n$ = 21) | Control ($n$ = 19) | $P$‡ |
|---|---|---|---|---|---|---|---|---|---|---|
| Transmembrane and coiled domain-containing protein | *C6orf129* | NM_138493 | 6p21.2 | Single-pass membrane protein | Unknown | No data | No data | 10 | 2 | 0.016 |
| Stathmin-like 4 | *STMN4* | NM_030795 | 8p21.2 | Intracellular | Intracellular signaling cascade | Brain | Neuronal and glial cells | 12 | 4 | 0.027 |
| Transmembrane protein 9 domain family, member B | *TMEM9B* | NM_020644 | 11p15.4 | Single-pass membrane protein | Signal transducer activity, positive regulation of 1κB/NF-κB cascade | Ubiquitous | No data | 9 | 2 | 0.034 |
| Fibroblast growth factor receptor 3 | *FGFR3* | NM_000142 | 4p16.3 | Single-pass membrane protein | JAK-STAT cascade, MAPKKK cascade, cell growth, FGFR signaling, protein amino acid phosphorylation, sensory perception of sound, skeletal system development | Ubiquitous; brain++ | Neuronal cells | 7 | 1 | 0.046 |
| Cleft lip and palate transmembrane protein 1 | *CLPTM1* | NM_001294 | 5p15.33 | Multi-pass membrane protein | Cell differentiation, multicellular organismal development, regulation of T-cell differentiation in thymus | Ubiquitous | Neuronal cells | 5 | 0 | 0.049 |
| EH-domain containing protein 1 | *EHD1* | NM_006795 | 11q13.1 | Cell membrane, endosome | Acts in early endocytic membrane fusion and membrane trafficking of recycling endosomes | Ubiquitous; immune cells | No data | 5 | 0 | 0.049 |
| Eukaryotic translation elongation factor 2 | *EEF2* | NM_001961 | 19p13.3 | Cytoplasmic | Protein biosynthesis | Ubiquitous | Brain | 5 | 0 | 0.049 |

* mRNA expression, data obtained from BioGPS (http://biogps.gnf.org).
† Protein expression, data obtained from www.proteinatlas.org.
‡ Fisher's two-sided exact test.

patients. $P < 0.05$ was considered statistically significant. Student's *t*-test was used to analyze the mean of the distribution of positives in serum screening and the mean distribution of age in patient cohorts. The Mann-Whitney test was used to analyze the difference in means of the ELISA reactivity of the PXFG serum versus the control serum.

## RESULTS

### Differential Autoantibody Expression between Control and PXFG Patients

To identify PXFG-associated disease markers, we screened the serum of 21 PXFG patients and 19 age- and sex-matched control individuals by using high-density colony macroarrays. The control and PEX glaucoma groups were age and sex matched. The control group consisted of 10 women and 9 men with a mean age of 73 ± 2.01 years, and the PXFG group consisted of 10 women and 11 men with a mean age of the 76.81 ± 1.90 years ($P = 0.18$).

We identified complex autoantibody repertoires in both the control and PXFG patients. The mean number of autoantigens scored was 1165 ± 196.5, with a wide variation in the count (range, 59–5442). The differences between the number of autoantigens in individual sera were independent of disease status. The mean number of autoantigens identified in the control and PXFG groups was 1240 ± 316.1 and 1091 ± 247.9, respectively ($P = 0.7107$).

Comparison of the autoantibody profiles between the PXFG and control groups identified nine clones that were significantly more prevalent in the PXFG group. After sequencing and analysis of the cDNA inserts of the clones, two were excluded because the cDNA was not within the open reading frame of a known protein. The cDNA of the remaining clones encoded for fragments or the full length of the following proteins: C6ORF129; stathmin-like 4 (STMN4); transmembrane protein 9 domain family, member B (TMEM9B); fibroblast growth factor receptor 3 (FGFR3); cleft lip and palate transmembrane protein 1 (CLPTM1); EH-domain-containing protein 1 (EHD1); and eukaryotic translation elongation factor 2 (EEF2). For each of these proteins, Table 2 shows the gene and cellular location, the function of the protein, and the number of positive PXFG and control patients. Figure 1 is a representation of these proteins, highlighting their conserved domains and the portion of the protein encoded by the clonal cDNA.

### C6ORF129 Levels in the Sera of Patients with PXFG

The most prevalent autoantigen in the PXFG patients compared with the control patients, C6ORF129, was selected for validation of the array results in a reverse ELISA. The protein was purified by affinity chromatography and gel filtration (Fig. 2). Sera from 26 patients with PXFG and sera from 20 control subjects were screened by reverse ELISA for reactivity with the purified C6orf129. Evaluation of the demographic data of the patients showed that the control and PXFG groups were sex matched. The control group consisted of 9 women and 11 men, and the PXFG group consisted of 13 women and 13 men. However, the PXFG group was slightly older (mean, 76.7 ± 1.8

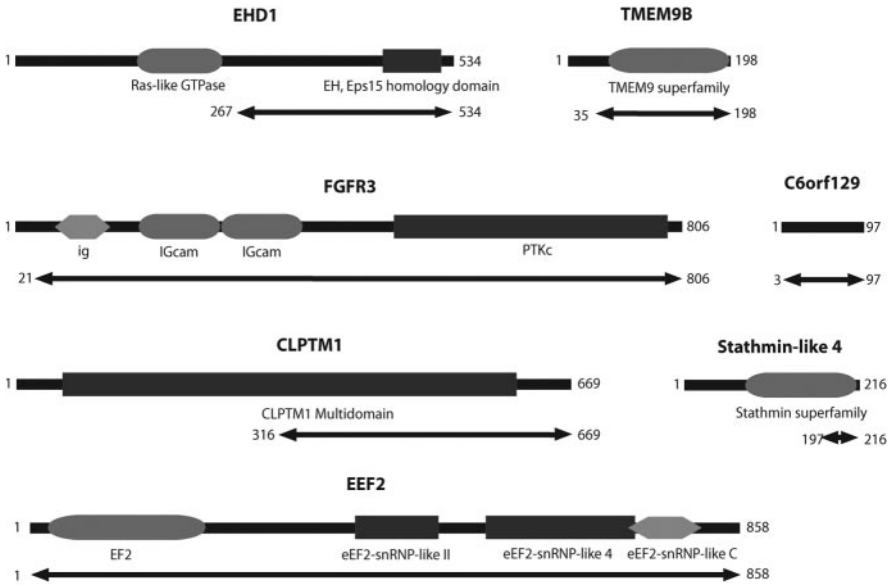


**FIGURE 1.** The antigens associated with PXFG glaucoma after screening of the sera of patients for IgG antibodies to recombinant protein expressed by cDNA clones with high-density colony macroarrays. The conserved domains of each antigen are highlighted, and the *arrows* indicate the length of the protein in amino acids that is encoded by the clone.

years) than the control group (mean, 67.4 ± 2.5 years; $P = 0.003$). There was no statistically significant correlation between the age of the patient and immunoreactivity to C6orf129 in both the control (Spearman correlation = 0.2836; $P = 0.26$) and PXFG (Spearman correlation = 0.26; $P = 0.19$) groups. Figure 3 shows the reverse ELISA data of the serum screened for autoantibodies to the recombinant C6ORF129 protein. The difference in the means between the PXFG group (0.53 ± 0.44 nm) and the control group (0.33 ± 0.45 nm) was statistically significant (Mann-Whitney test $P = 0.007$).

### Antigens at the mRNA Level in RGC-5 Cells and in cDNA from Human Brain and Optic Nerve

We next performed a qPCR analysis to determine the expression of the antigens identified in a rat retinal ganglion cell line (RGC-5). With the exception of STMN4, we found that all antigens were expressed in rat RGC-5 cells (Fig. 4A). Furthermore, using cDNA from human brain and optic nerve, we confirmed the presence of all antigens in human brain and optic nerve (Figs. 4B, 4C). The lack of specific antibodies to several of the antigens did not permit the analysis of antigen expression on a protein level.

## DISCUSSION

Several investigators have reported the presence of autoantibodies in glaucoma patients.[19–28,36–38] In most of the studies, sera from patients with glaucoma and normal control subjects were tested against Western blots of ocular antigens and the IgG patterns analyzed by multivariate statistical techniques. Subsequent statistically significant antigens were identified by mass spectrometry. This method is biased toward the identification of autoantibodies directed against antigens that have a high level of expression. In comparison, protein arrays repre-

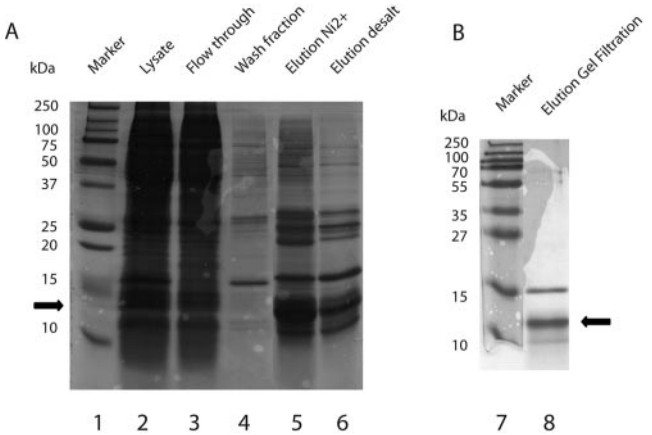


**FIGURE 2.** Coomassie-stained 15% SDS-PAGE analysis of expression and purification of C6orf129. (**A**) *Lane 1*: molecular marker; *lane 2*: supernatant of lysate loaded onto $Ni^{2+}$ affinity column; *lane 3*: flow through fraction from $Ni^{2+}$ affinity column; *lane 4*: wash fraction at 20 mM imidazole from $Ni^{2+}$ affinity column; *lane 5*: elution fraction at 250 mM imidazole from $Ni^{2+}$ affinity column; *lane 6*: elution fraction from HiTrap desalting column. (**B**) *Lane 7*: molecular marker; *lane 8*: protein from the gel-filtration column. *Arrow*: expected size of the recombinant C6orf129.

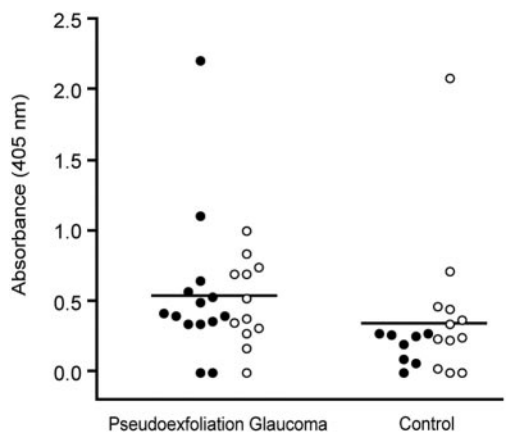


**FIGURE 3.** Serum IgG reactivity of 26 patients with PXFG and 20 patient control subjects against purified recombinant C6orf129 protein using reverse ELISA. The data show the absorbance for each patient's serum, which was calculated by subtracting the absorbance of the well containing no C6ORF129 from the well containing C6ORF129. (○) Patients who were screened on the original protein array study; (●) new patients. Bar, mean value of each group. The difference between the PXFG group (0.5348) and the control group (0.3343) means was statistically significant (Mann-Whitney test $P = 0.0069$).

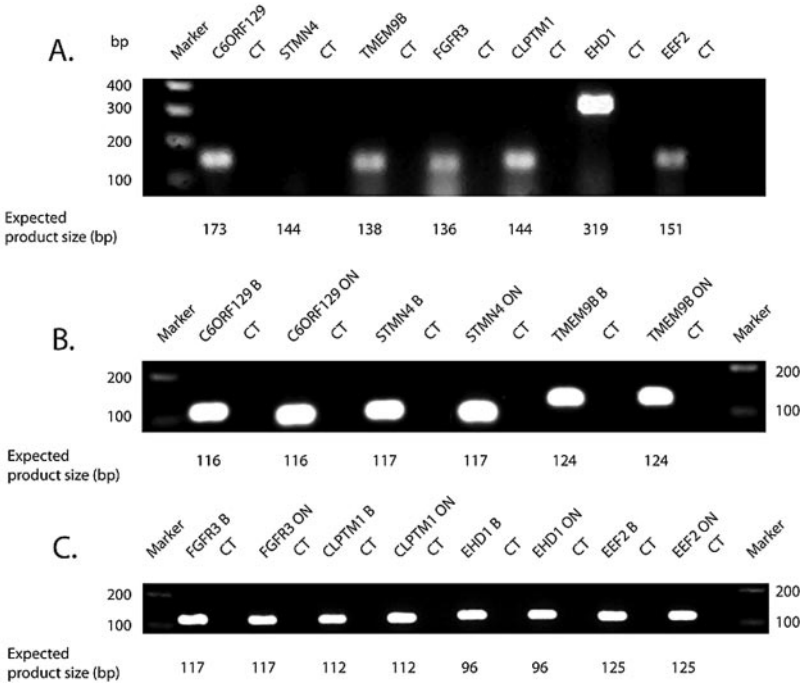


**FIGURE 4.** Expressional analysis of genes associated with PXFG. (**A**) Total RNA was isolated from RGC-5 cells, reverse transcribed, and subjected to PCR with gene-specific primers. All genes associated with PXFG except for *STMN4* are expressed in RGC-5 cells. cDNA from (**B**, **C**) human brain (B) and optic nerve (ON) was examined for the presence of all genes associated with PXFG and found to be present in both. The negative control (CT) is to the *right* for each gene.

sent an alternative approach to identifying potential markers in a high-throughput manner, as more than 10,000 different proteins can be analyzed simultaneously. This method enables the detection of autoantigens regardless of the level of expression in their native host tissue. It also allows for the straightforward molecular cloning of genes that encode for the autoantigen.

Complex, widely diversified autoantibody repertoires are present in seemingly healthy people.[39,40] Because of the diversity, a large number of patients must be screened to find disease-specific proteins. This diversity is also seen in the different glaucoma groups, with a different pattern of autoantibodies among patients with primary open-angle glaucoma, ocular hypertension, and normal-tension glaucoma. The divergent patterns may represent individual differences and/or the multifactorial nature of the etiology of glaucoma. To potentially limit some of these differences, we selected patients with a known secondary cause of their glaucoma who were likely to have the same mechanism of injury to the optic nerve. We did not find any of the autoantibodies in the previous studies to be more prevalent in PXFG than in the control subjects. This finding could be due to the different techniques used and/or the different sample population, as the previous autoimmune studies in glaucoma have concentrated on POAG and NTG.

The biological role of these antibodies and their corresponding antigens is not clear. There is still some debate on whether this activated response is neuroprotective or neurodestructive. An induced T-cell autoimmune response has been shown to protect against progression of glaucomatous optic nerve damage in animal experimental models.[10] However, exogenously applied antibodies against Hsp27 and γ-enolase identified in previous autoantibody glaucoma studies have been shown to facilitate apoptotic cell death in retinal ganglion cells.[25,38,41] Furthermore, it has been observed that the hsp27 enters neuronal and glial cells in human retina by an endocytic mechanism and thereby facilitates apoptotic cell death.[41] Further investigations are needed to assess whether the autoantibodies or corresponding antigens identified in our study relate to the molecular pathogenesis of glaucoma or PXF.

Initial validation of the array data was provided by demonstrating greater immunoreactivity to C6orf129 in the serum of PXFG patients than in that of control subjects. The PXFG group was slightly older than the control population (mean difference, 9 years) which is a reflection of the difficulty of recruiting control patients in this age group without any ocular disease or diabetes mellitus. Given that there was no significant correlation between age and immunoreactivity, this age difference is unlikely to have an effect on the result. It is not known whether this immune response is specific to PXF, part of a generalized response to the optic neuropathy, or due to a systemic condition that is more common in the PXFG group. Further reverse ELISAs of sera from a larger cohort of patients with PXF, PXFG, POAG, OHT, and NTG may provide further data as to the specificity of the autoimmune response to C6orf129, rule out any age correlation, and further characterize its potential role as a biomarker.

C6orf129 encodes for a novel protein with a transmembrane domain. It is conserved in chimpanzee, dog, cow, rat, and chicken. To date, there is no expression data at the mRNA or protein level. Further investigation as to the role of this protein should include examining mRNA expression levels in various tissues and the production of an antibody to study protein expression. Also the effect of mRNA expression levels in the RGC-5 cells after various stimuli could be studied.

Further validation of the array data was provided by demonstrating that the antigens, apart from STMN4 in the RGC-5 cells, were expressed at the mRNA level in the RGC-5 cell line and in human brain and optic nerve. The expression of STMN4 has been shown in the retinal ganglion cell layer and is increased after optic nerve injury.[42,43] Therefore, it may require the application of a stimulus to be detected in the RGC-5 cells. Also, RGC-5 is an immortalized cell line and, as such, can be very different from the original cells used. Our results may simply reflect the limitations of the cell line.

A potential functional role in neuronal survival and growth for some of the antigens has been suggested by some studies. FGFR3 is upregulated after peripheral nerve lesions in mice,[44] and FGFR3-deficient mice are resistant against lesion-induced neuron loss.[45] TMEM9B expression is essential for the production of proinflammatory cytokines induced by tumor necrosis factor (TNF).[46] Retinal ganglion cells are susceptible targets of TNF-α mediated death signaling.[47–49] Aging Stathmin$^{-/-}$ mice develop axonopathy in the central nervous system, optic

nerve, and peripheral nervous system.[50] EEF2 is involved in the regulation of neurite outgrowth by a calcium-induced inhibition of EEF2.[51]

The potential role of the antigens in the molecular mechanisms responsible for pathogenesis of PXF syndrome and its associated glaucoma is not clear. Basic fibroblast growth factor, a ligand for FGFR3, has been shown to be elevated in the aqueous humor of PXF patients with and those without glaucoma.[52] A polymorphism in the *TNFa* gene, which interacts with *TMEM9B*, has been identified to be strongly associated with PXFG.[53] Polymorphisms in the *LOXL1* gene has been identified as a major genetic risk factor for PXF.[9] However, a large proportion of the unaffected control subjects also carry the high-risk haplotype. Therefore, additional factors must be necessary to trigger the abnormal fibrillar production. Data suggest that there is vesicular transport of *LOXL1* to the cellular surface, where it immediately associates with microfibrillar structures to participate in the formation of PXF fibrils.[54] Several of the antigens identified are transmembrane proteins (C6orf129, FGFR3, CLPTM1, TMEM9B, and EHD1) that may offer the potential for further investigation into possible interactions with the LOXL1 enzyme.

It remains to be investigated whether the antibodies in serum identified in the present study cause or have a strong influence on glaucomatous optic neuropathy or PXF. Although, these antibodies may not be directly responsible for the disease, they could be useful as biomarkers, either individually or in a panel, to aid in the diagnosis and monitoring of glaucoma. They also may provide novel therapeutic targets for the specific prevention of retinal neural degeneration in glaucoma patients.

## *Acknowledgments*

The authors thank Tom Wall and Imran Hassan for their contributions and Beau Fenner for helpful suggestions and criticism.

## *References*

1. Bourne RR. Worldwide glaucoma through the looking glass. *Br J Ophthalmol.* 2006;90:253–254.
2. Quigley HA, Broman AT. The number of people with glaucoma worldwide in 2010 and 2020. *Br J Ophthalmol.* 2006;90:262–267.
3. Schlotzer-Schrehardt U, Naumann GO. Ocular and systemic pseudoexfoliation syndrome. *Am J Ophthalmol.* 2006;141:921–937.
4. Ritch R, Schlotzer-Schrehardt U, Konstas AG. Why is glaucoma associated with exfoliation syndrome? *Prog Retin Eye Res.* 2003; 22:253–275.
5. Cahill M, Early A, Stack S, Blayney AW, Eustace P. Pseudoexfoliation and sensorineural hearing loss. *Eye.* 2002;16:261–266.
6. Janciauskiene S, Krakau T. Alzheimer's peptide and serine proteinase inhibitors in glaucoma and exfoliation syndrome. *Doc Ophthalmol.* 2003;106:215–223.
7. Linner E, Popovic V, Gottfries CG, Jonsson M, Sjogren M, Wallin A. The exfoliation syndrome in cognitive impairment of cerebrovascular or Alzheimer's type. *Acta Ophthalmol Scand.* 2001;79:283–285.
8. Mitchell P, Wang JJ, Smith W. Association of pseudoexfoliation syndrome with increased vascular risk. *Am J Ophthalmol.* 1997; 124:685–687.
9. Thorleifsson G, Magnusson KP, Sulem P, et al. Common sequence variants in the LOXL1 gene confer susceptibility to exfoliation glaucoma. *Science.* 2007;317:1397–1400.
10. Schwartz M, London A. Glaucoma as a neuropathy amenable to neuroprotection and immune manipulation. *Prog Brain Res.* 2008; 173:375–384.
11. Ahmed F, Brown KM, Stephan DA, Morrison JC, Johnson EC, Tomarev SI. Microarray analysis of changes in mRNA levels in the rat retina after experimental elevation of intraocular pressure. *Invest Ophthalmol Vis Sci.* 2004;45:1247–1258.
12. Miyahara T, Kikuchi T, Akimoto M, Kurokawa T, Shibuki H, Yoshimura N. Gene microarray analysis of experimental glaucomatous retina from cynomolgus monkey. *Invest Ophthalmol Vis Sci.* 2003;44:4347–4356.
13. Yang Z, Quigley HA, Pease ME, et al. Changes in gene expression in experimental glaucoma and optic nerve transection: the equilibrium between protective and detrimental mechanisms. *Invest Ophthalmol Vis Sci.* 2007;48:5539–5548.
14. Tezel G. The role of glia, mitochondria, and the immune system in glaucoma. *Invest Ophthalmol Vis Sci.* 2009;50:1001–1012.
15. Neufeld AH. Microglia in the optic nerve head and the region of parapapillary chorioretinal atrophy in glaucoma. *Arch Ophthalmol.* 1999;117:1050–1056.
16. Yang J, Yang P, Tezel G, Patil RV, Hernandez MR, Wax MB. Induction of HLA-DR expression in human lamina cribrosa astrocytes by cytokines and simulated ischemia. *Invest Ophthalmol Vis Sci.* 2001;42:365–371.
17. Yang J, Patil RV, Yu H, Gordon M, Wax MB. T cell subsets and sIL-2R/IL-2 levels in patients with glaucoma. *Am J Ophthalmol.* 2001;131:421–426.
18. Tezel G, Wax MB. The immune system and glaucoma. *Curr Opin Ophthalmol.* 2004;15:80–84.
19. Grus FH, Joachim SC, Hoffmann EM, Pfeiffer N. Complex autoantibody repertoires in patients with glaucoma. *Mol Vis.* 2004;10: 132–137.
20. Joachim SC, Grus FH, Pfeiffer N. Analysis of autoantibody repertoires in sera of patients with glaucoma. *Eur J Ophthalmol.* 2003; 13:752–758.
21. Wax MB, Tezel G, Kawase K, Kitazawa Y. Serum autoantibodies to heat shock proteins in glaucoma patients from Japan and the United States. *Ophthalmology.* 2001;108:296–302.
22. Wax MB, Tezel G, Saito I, et al. Anti-Ro/SS-A positivity and heat shock protein antibodies in patients with normal-pressure glaucoma. *Am J Ophthalmol.* 1998;125:145–157.
23. Yang J, Tezel G, Patil RV, Romano C, Wax MB. Serum autoantibody against glutathione S-transferase in patients with glaucoma. *Invest Ophthalmol Vis Sci.* 2001;42:1273–1276.
24. Grus FH, Joachim SC, Bruns K, Lackner KJ, Pfeiffer N, Wax MB. Serum autoantibodies to alpha-fodrin are present in glaucoma patients from Germany and the United States. *Invest Ophthalmol Vis Sci.* 2006;47:968–976.
25. Maruyama I, Ohguro H, Ikeda Y. Retinal ganglion cells recognized by serum autoantibody against gamma-enolase found in glaucoma patients. *Invest Ophthalmol Vis Sci.* 2000;41:1657–1665.
26. Tezel G, Edward DP, Wax MB. Serum autoantibodies to optic nerve head glycosaminoglycans in patients with glaucoma. *Arch Ophthalmol.* 1999;117:917–924.
27. Joachim SC, Reichelt J, Berneiser S, Pfeiffer N, Grus FH. Sera of glaucoma patients show autoantibodies against myelin basic protein and complex autoantibody profiles against human optic nerve antigens. *Graefes Arch Clin Exp Ophthalmol.* 2008;246:573–580.
28. Reichelt J, Joachim SC, Pfeiffer N, Grus FH. Analysis of autoantibodies against human retinal antigens in sera of patients with glaucoma and ocular hypertension. *Curr Eye Res.* 2008;33:253–261.
29. Bussow K, Nordhoff E, Lubbert C, Lehrach H, Walter G. A human cDNA library for high-throughput protein expression screening. *Genomics.* 2000;65:1–8.
30. Kijanka G, Murphy D. Protein arrays as tools for serum autoantibody marker discovery in cancer. *J Proteomics.* 2009;72:936–944.
31. Horn S, Lueking A, Murphy D, et al. Profiling humoral autoimmune repertoire of dilated cardiomyopathy (DCM) patients and development of a disease-associated protein chip. *Proteomics.* 2006;6: 605–613.
32. Kijanka G, Hector S, Kay EW, et al. Human IgG antibody profiles differentiate between symptomatic patients with and without colorectal cancer. *Gut.* 2010;59(1):69–78.
33. The Guidelines Task Force. *Terminology and Guidelines for Glaucoma.* 3rd ed. The European Glaucoma Society; 2008.
34. Bussow K, Cahill D, Nietfeld W, et al. A method for global protein expression and antibody screening on high-density filters of an arrayed cDNA library. *Nucleic Acids Res.* 1998;26:5007–5008.

35. Altschul SF, Gish W, Miller W, Myers EW, Lipman DJ. Basic local alignment search tool. *J Mol Biol.* 1990;215:403–410.
36. Joachim SC, Pfeiffer N, Grus FH. Autoantibodies in patients with glaucoma: a comparison of IgG serum antibodies against retinal, optic nerve, and optic nerve head antigens. *Graefes Arch Clin Exp Ophthalmol.* 2005;243:817–823.
37. Romano C, Barrett DA, Li Z, Pestronk A, Wax MB. Anti-rhodopsin antibodies in sera from patients with normal-pressure glaucoma. *Invest Ophthalmol Vis Sci.* 1995;36:1968–1975.
38. Tezel G, Seigel GM, Wax MB. Autoantibodies to small heat shock proteins in glaucoma. *Invest Ophthalmol Vis Sci.* 1998;39:2277–2287.
39. Li WH, Zhao J, Li HY, et al. Proteomics-based identification of autoantibodies in the sera of healthy Chinese individuals from Beijing. *Proteomics.* 2006;6:4781–4789.
40. Avrameas S. Natural autoantibodies: from 'horror autotoxicus' to 'gnothi seauton'. *Immunol Today.* 1991;12:154–159.
41. Tezel G, Wax MB. The mechanisms of hsp27 antibody-mediated apoptosis in retinal neuronal cells. *J Neurosci.* 2000;20:3552–3562.
42. Nakazawa T, Morii H, Tamai M, Mori N. Selective upregulation of RB3/stathmin4 by ciliary neurotrophic factor following optic nerve axotomy. *Brain Res.* 2005;1061:97–106.
43. Nakazawa T, Nakano I, Furuyama T, Morii H, Tamai M, Mori N. The SCG10-related gene family in the developing rat retina: persistent expression of SCLIP and stathmin in mature ganglion cell layer. *Brain Res.* 2000;861:399–407.
44. Grothe C, Meisinger C, Hertenstein A, Kurz H, Wewetzer K. Expression of fibroblast growth factor-2 and fibroblast growth factor receptor 1 messenger RNAs in spinal ganglia and sciatic nerve: regulation after peripheral nerve lesion. *Neuroscience.* 1997;76:123–135.
45. Jungnickel J, Klutzny A, Guhr S, Meyer K, Grothe C. Regulation of neuronal death and calcitonin gene-related peptide by fibroblast growth factor-2 and FGFR3 after peripheral nerve injury: evidence from mouse mutants. *Neuroscience.* 2005;134:1343–1350.
46. Dodeller F, Gottar M, Huesken D, Iourgenko V, Cenni B. The lysosomal transmembrane protein 9B regulates the activity of inflammatory signaling pathways. *J Biol Chem.* 2008;283:21487–21494.
47. Tezel G, Li LY, Patil RV, Wax MB. TNF-alpha and TNF-alpha receptor-1 in the retina of normal and glaucomatous eyes. *Invest Ophthalmol Vis Sci.* 2001;42:1787–1794.
48. Tezel G, Wax MB. Increased production of tumor necrosis factor-alpha by glial cells exposed to simulated ischemia or elevated hydrostatic pressure induces apoptosis in cocultured retinal ganglion cells. *J Neurosci.* 2000;20:8693–8700.
49. Tezel G, Yang X, Yang J, Wax MB. Role of tumor necrosis factor receptor-1 in the death of retinal ganglion cells following optic nerve crush injury in mice. *Brain Res.* 2004;996:202–212.
50. Liedtke W, Leman EE, Fyffe RE, Raine CS, Schubart UK. Stathmin-deficient mice develop an age-dependent axonopathy of the central and peripheral nervous systems. *Am J Pathol.* 2002;160:469–480.
51. Iizuka A, Sengoku K, Iketani M, et al. Calcium-induced synergistic inhibition of a translational factor eEF2 in nerve growth cones. *Biochem Biophys Res Commun.* 2007;353:244–250.
52. Gartaganis SP, Georgakopoulos CD, Exarchou AM, Mela EK, Lamari F, Karamanos NK. Increased aqueous humor basic fibroblast growth factor and hyaluronan levels in relation to the exfoliation syndrome and exfoliative glaucoma. *Acta Ophthalmol Scand.* 2001;79:572–575.
53. Khan MI, Micheal S, Rana N, et al. Association of tumor necrosis factor alpha gene polymorphism G-308A with pseudoexfoliative glaucoma in the Pakistani population. *Mol Vis.* 2009;15:2861–2867.
54. Schlotzer-Schrehardt U. Molecular pathology of pseudoexfoliation syndrome/glaucoma: new insights from LOXL1 gene associations. *Exp Eye Res.* 2009;88:776–785.